MAJOR PAPER

Giant Cell Tumors of the Bone: Changes in Image Features after Denosumab Administration

Sota Oguro[1*], Shigeo Okuda[1], Hiroaki Sugiura[1], Shunsuke Matsumoto[1],
Aya Sasaki[2], Michiro Susa[3], Hideo Morioka[4], and Masahiro Jinzaki[1]

Purpose: To assess the clinical importance in the feature change in giant cell tumors of the bone (GCTB) after denosumab treatment, detected by MRI.

Methods: In 12 patients, MRI and CT of GCTB obtained before and after the treatment retrospectively compared. The tumor size, the signal intensity (SI) ratio between the solid part of the GCTB and muscle, cystic part size, gadolinium enhancement and apparent diffusion coefficient (ADC) value were measured on MRI. The bone formation in the tumor was observed on CT and X-ray.

Results: The mean number of denosumab injections was 19 ± 10. The follow-up period was up to 2 years. One case showed partial remission, while the other 11 cases were stable. A mean SI ratio on T_2-weighted image statistically significantly decreased from 3.9 to 1.9 after the treatment. A cystic component in the tumor was observed in five cases before the treatment, and the diameter of the cystic part decreased after the treatment in 80% of cases (4/5). All the tumors showed contrast enhancement on T_1-weighted image pre- and post-treatment (11/11). The averaged ADC values were 1.52×10^{-3} mm^2/s before and 1.44×10^{-3} mm^2/s after the treatment ($P = 0.63$). Bone formation in the tumor was observed in 58% of cases (7/12).

Conclusion: The decrease of SI ratio on T_2-weighted image, shrinkage of cystic part and bone formation should be regarded as the effectiveness of denosumab treatment despite of no substantial change in the tumor size.

Keywords: *denosumab, giant cell tumor of bone, magnetic resonance imaging*

Introduction

Giant cell tumors of the bone (GCTB) typically exhibit osteolytic changes in the epiphyseal or apophyseal region of long bones. Surgical resection and filling with polymethylmethacrylate cement is the standard treatment when treating these osteolytic lesions as resectable tumors. Medical treatments that use bisphosphonates have been proposed as a therapeutic option in cases with metastatic or unresectable disease to reduce osteoclast activity.[1] More recently, denosumab

[1]Radiology Department, School of Medicine, Keio University, 35 Shinanomachi, Shinjuku, Tokyo 160-8582, Japan
[2]Pathology Department, School of Medicine, Keio University, Tokyo, Japan
[3]Department of Orthopaedic Surgery, National Defense Medical College Hospital, Saitama, Japan
[4]Department of Orthopaedic Surgery, School of Medicine, Keio University, Tokyo, Japan
*Corresponding author, Phone: +81-3-3353-1211, Fax: +81-3-3353-1977, E-mail: soguro@rad.med.keio.ac.jp

(Ranmark; Daiichi Sankyo Company, Ltd., Tokyo, Japan) has been approved to treat GCTB.[2] Denosumab is a human monoclonal antibody that targets the receptor activator of nuclear factor-κB ligand (RANKL) with high specificity and affinity.[3] Receptor activator of nuclear factor kappa-B ligand is a signaling molecule that is required for the bone resorptive function of osteoclast-like cells and is highly expressed on the stromal cells of tumors.[4,5] Denosumab reduces the activity of osteoclast-like cells by blocking RANKL and has been shown to be effective in combatting bone metastasis or multiple myeloma in several reports.[6–8] Branstetter et al. reported that in patients with GCTB, denosumab treatment reduced the relative content of some phenotypes when viewed under histology.[9] These included proliferative, densely cellular tumor stromal cells, which were replaced with non-proliferative, differentiated, and densely woven new bone. It has been stated to be important to evaluate the metabolic changes occurred in tumor than tumor shrinkage.[10] Moreover, MRI has been more frequently used for tumor response evaluation, because they provide detailed anatomic, and functional, or metabolic change information during tumor treatment. Although the new bone formation may be visualizable on X-ray or CT

images within the tumor, disruption of tumor progression evaluated using MRI might be a more appropriate indicator of improvement in patient outcome. Additionally, several studies reported that apparent diffusion coefficient (ADC) values could reflect the immunohistochemical features of a specific tumor and could then more precisely predict the aggressiveness and potential response of a particular tumor prior to initializing treatment.[11,12] The purpose of this study was, therefore, to assess the clinical importance in the feature change in GCTB after denosumab treatment, detected by MRI.

Materials and Methods

Denosumab treatment and study population
The Institutional Review Board of our hospital approved this retrospective study. The requirement for informed patient consent was waived for this study. The inclusion criteria in this study for denosumab treatment were the following: adults who weighed at least 45 kg with lesions that were histologically confirmed as GCTB. The exclusion criteria were the following: a diagnosis of a second malignancy within the past 5 years, a history or current evidence of osteonecrosis or osteomyelitis of the jaw, active dental or jaw conditions necessitating oral surgery, and pregnancy. Denosumab (40 mg) was injected every 4 weeks. Vitamin D and calcium were prescribed for all patients.[13]

The study included 12 patients with GCTB who were treated with denosumab from November 2011 to August 2014 in our hospital. There were seven male and five female patients. The patients had a mean age with standard deviation of 41 ± 12 years old (range, 26–66 years old). All patients were histologically diagnosed after biopsy at our institution. In this series, six cases of recurrent GCTB were included after initial treatment except denosumab. The mean number of denosumab injections was 19 ± 10 (mean ± range).

Image analysis
For this study, pre-therapeutic and post-therapeutic images were compared in all cases. The pre-therapeutic images were obtained within 1 month before the initial denosumab treatment. The post-therapy images were obtained at least 10 months after the initial denosumab treatment. The mean observation period was 19.8 months, and the median observation period was 18 months.

The MRI was performed using a 1.5T MR scanner (Signa HD; GE Healthcare, Waukesha, WI, USA). The T_2-weighted images were obtained with the following parameters: TR/TE, 2,000–4,600/70–100 ms; slice thickness, 3–5 mm; interslice gap, 0.3–1 mm; and FOV, 140–240 mm. The tumor size was measured on T_2-weighted axial image and compared between pre- and post-treatment using the response evaluation criteria in solid tumors (RECIST) scale.[14] To assess the solid part of the tumor, the signal intensity (SI) ratio between the solid part of the GCTB and muscle (tumor SI/muscle SI) on a T_2-weighted image was evaluated.[15,16] The region of interest was drawn manually at the center of the solid part of the GCTB, avoiding strong calcification or bone marrow formation. The size of the ROI was from 3 to 9 mm. Then, the size of the cystic component (indicated by aneurysmal bone cyst-like changes) was measured on pre- and post-treatment T_2-weighted image.[17] The maximum diameter of cystic lesion was measured as a reference. In case of a multilocular cystic lesion, the largest diameter of entire cystic mass was measured. If there were more than one cystic mass, the largest cystic lesion was selected as the measuring target. Then, T_1-weighted images with fat suppression (FsT_1WI) were obtained using gradient echo T_1-weighted images with the following parameters: TR/TE, 170–240 m/1.7–2.6 ms, flip angle 90°, slice thickness 3–5 mm with no inter-slice gap, FOV 140–240 mm and the matrix was 320×192. In 11 of 12 patients, contrast-enhanced FsT_1WI was obtained following the administration of meglumine gadopentetate (Magnevist, Bayer Yakuhin, Ltd., Osaka, Japan), in a dose of 0.2 mL/kg by hand injection into a median cubital vein. In one patient, contrast-enhanced images were not obtained due to the contraindication for using contrast material. Next, diffusion-weighted images were obtained in all patients who have not undertaken any pretreatment, using the following parameters: b value, $1,000 \text{ s/mm}^2$; slice thickness, 5–6 mm; TR/TE, 4,000–6,000/72–96 m; acquisition matrix, 160×128; number of acquisitions, 6–8. An ADC map was generated using a workstation software (Advantage Workstation 4.3, GE Healthcare, Waukesha, WI, USA), and the ROI was placed in the solid part of the tumor on the map to measure the ADC value.[18] Computed tomography and X-ray were referred for evaluating new bone formation after treatment with denosumab.[9] The two radiologists had consensus regarding the measurements of the tumor size, the size of the cystic lesion, the location and size of the ROI on T_2WI and ADC map.

Pre- and post-treatment measurements of tumor diameter, the size of the cystic component, ADC values were compared using Student's t-test. A value of $P < 0.05$ was considered to indicate statistical significance.

Results

The characteristics of the patients are shown in Table 1. Mean pre- and post-treatment tumor size significantly decreased from 47.1 ± 22.6 to 40.6 ± 21.8 mm ($P = 0.01$), respectively. One case showed more than a 30% reduction in size (partial remission), and the other cases were assessed as stable disease. The SI ratio between the solid part of the tumor and the muscle was 3.9 ± 3.1 and decreased to 1.9 ± 0.9 after denosumab treatment, which was statistically significant ($P = 0.036$). A cystic component was observed in the tumor in five out of six cases who have not undertaken pretreatment, and the diameter of the cystic formation was decreased in 4/5 cases (80%). In these five cases with cystic

Table 1 Short-term imaging findings in patients with giant cell tumors of the bone who were treated with denosumab

No.	Sex	Age	Location	Pretreatment	Tumor size (mm)		Size of cystic component (mm)		SI ratio on T_2 weighted image		New bone formation	ADC value ($10^{-3} \times$ mm²/sec)	
					Pre	Post	Pre	Post	Pre	Post		Pre	Post
1	M	37	Tibia	–	60	50	43	18	3.6	2.9	+	1.03	0.66
2	M	26	Humerus	–	66	55	39	15	9.7	3.6	+	1.55	1.33
3	M	33	Carpus	–	25	22	10	0	4.9	1.1	+	1.25	1.29
4	M	52	Vertebra	–	32	30	15	15	10.7	0.9	+	1.66	2.24
5	M	41	Skull bone	–	46	20	40	12	3.5	2.7	–	2.60	1.74
6	F	34	Vertebra	–	23	22	0	0	2.2	1.7	+	0.91	1.23
7	M	54	Radius	Curettage with bone grafting	25	24	0	0	1.2	1.1	+	N/A	N/A
8	M	34	Femur	Curettage with bone grafting	64	60	0	0	1.3	0.8	+	N/A	N/A
9	F	26	Vertebra	Curettage alone	89	87	0	0	2.4	1.6	–	N/A	N/A
10	F	51	Vertebra	Curettage alone	30	24	0	0	2.2	1.3	–	N/A	N/A
11	F	39	Vertebra	Curettage alone	31	30	0	0	2.2	1.7	–	N/A	N/A
12	F	66	Sacrum	Embolization	74	63	0	0	3.4	3	–	N/A	N/A

ADC, apparent diffusion coefficient; SI ratio, the signal intensity ratio between the solid part of the tumor and muscle.

component, the mean diameter of the cystic component significantly decreased from 24.5 ± 18.4 to 12.9 ± 11.1 mm ($P = 0.02$). A cystic component was not observed in any recurrent cases. Moreover, the appearance of new cystic lesion was not revealed. All tumors were demonstrated in homogeneous hypointensity on FsT_1WI before the treatment. Marked enhancement was observed at the solid part of the tumor both pre- and post-treatment in seven patients. In one patient, the marked enhancement was changed to mild one due to strong calcification after the treatment. In three patients, the tumors were mildly enhanced before and after the treatments. The mean ADC value of the solid part of the tumor changed from 1.50 to 1.41×10^{-3} mm²/s, which was not statistically significant ($P = 0.70$). A representative example of an MRI is shown in Fig. 1. New bone formation in the tumor appeared on CT and X-ray images in seven of 12 cases (58%). Interestingly, five of six cases (83%) without pretreatment showed new bone formation, which was higher rate than recurrent cases 2/6 (33%). A representative example of new bone formation is shown in Fig. 2.

Discussion

In this report, we describe changes that were observed in GCTB imaging after denosumab treatment. After treatment with denosumab, GCTB was primarily observed using CT and MRI for approximately 20 months. Mean tumor size significantly decreased in these patients. Additionally, one case showed partial remission, while others achieved stable

disease. Branstetter et al. reported that in histological analyses, 65% of their patients exhibited an increase in the proportion of dense fibro-osseous tissue and/or new woven bone after denosumab treatment.[9] In our study, 58% of the cases showed bone formation in the tumor, a result that was comparable to those reported in previous reports. In the five patients who did not show new bone formation in the tumor, the lesion was located in the vertebrae in three cases, the sacrum in one case and the skull in one case. Lesions situated in the axial skeleton may have a reduced tendency to develop new bone formations within the tumor. On the other hand, four out of six cases were post-treatment. Pre-treatment, such as operation or embolization might affect the development of new bone formation. In our study, the region showing a cystic appearance in the tumor was significantly smaller after denosumab treatment. Sabokbar et al.[19] reported that macrophage-osteoclast differentiation may play a role in osteolysis and therefore, be associated with the enlargement of subchondral cysts in osteoarthritis. We hypothesized that the reduction of the cystic component in the GCTB following denosumab treatment might have been mediated by its blocking effect on RANKL, which could result in the suppression of osteoclasts.

In this study, we found the significant decrease in T_2WI SI ratio after the treatment. Dense calcification induced by the denosumab might contribute the signal decrease. Moreover, the number is reduced after the treatment in both multinucleated giant cells and intervening mononuclear cells, which are abundant in giant cell tumors, and the tumor
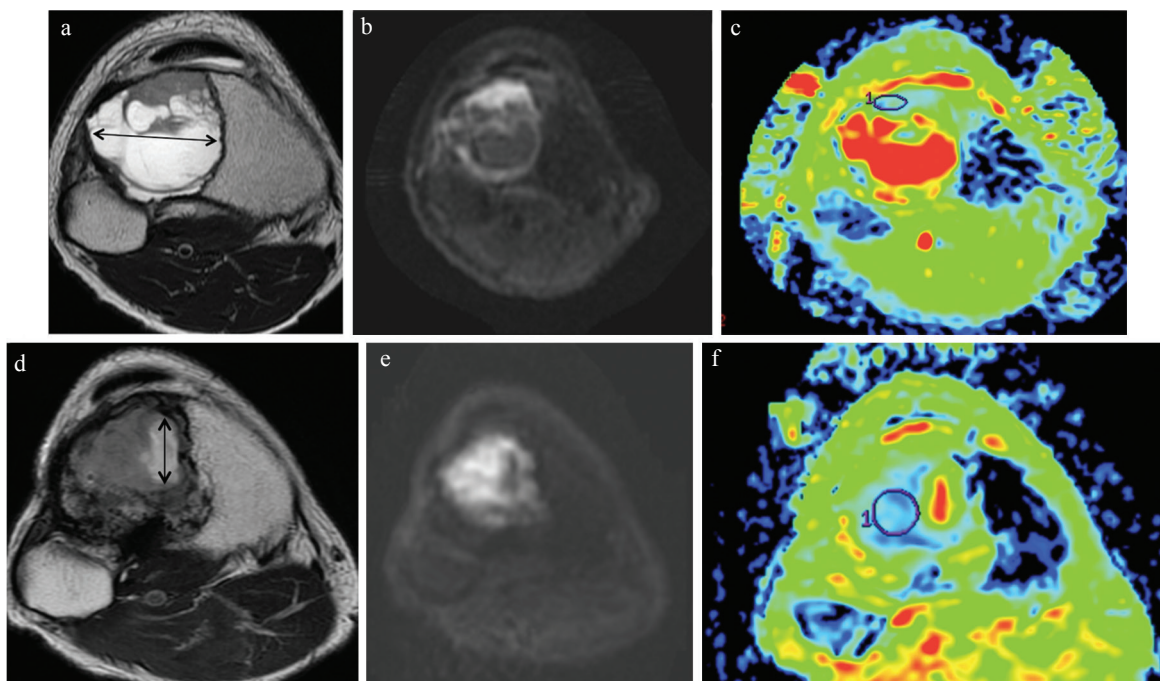
Fig. 1 Magnetic resonance images of tissues obtained from a 37 y/o male with giant cell tumors of the bone (GCTB) in the tibia. Images are shown before and after denosumab administration. (**a**) T_2-weighted image of a MRI showing GCTB exhibiting a cystic component in the proximal tibia. The tumor was 60 mm in size, including the cystic component. The cystic component was 43 mm in diameter. (**b** and **c**) On diffusion weighted image, the solid part of the tumor showed high intensity. On apparent diffusion coefficient (ADC) map (b = 1,000), the ADC value of the solid part of the tumor was 1.03 ($\times 10^{-3}$ mm^2/s). (**d**) T_2-weighted image after denosumab treatment showing that the tumor had decreased in size to 50 mm. The size of cystic component was 18 mm (double-headed arrow). (**e** and **f**) On diffusion weighted image, the solid part of the tumor showed high intensity. On ADC map (b = 1,000), the ADC value of the solid part of the tumor decreased to 0.66 ($\times 10^{-3}$ mm^2/s).
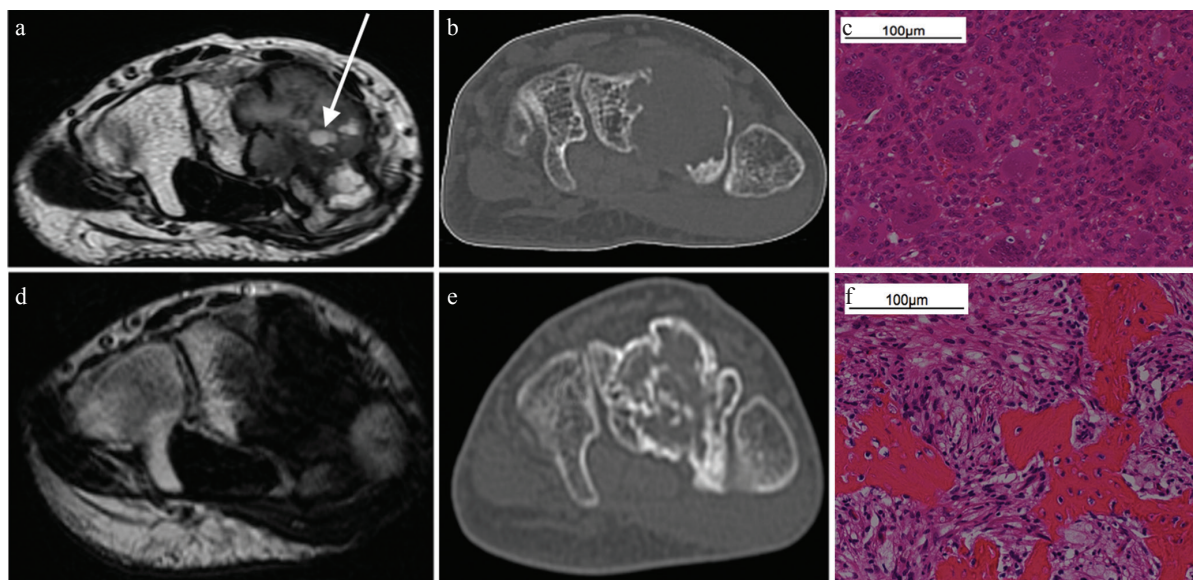

Fig. 2 Computed tomography and MRI of a 33 y/o male with giant cell tumors of the bone (GCTB) in the carpal bones. Images are shown before and after denosumab treatment. (**a** and **b**) The tumor exhibited a well-defined geographic lucent lesion in the carpal bones that was 25 mm in size. On T_2-weighted axial imaging, the tumor demonstrated well-circumscribed inhomogeneous hypo-intensity and a small cystic component (arrow). Computed tomography did not show bone formation in the tumor. (**c**) Both multinucleated giant cells and intervening mononuclear cells were observed in this photomicrograph. (**d** and **e**) On T_2-weighted axial imaging, the tumor exhibited inhomogeneous hypo-intensity with an unclear boundary. The small cystic component disappeared after treatment. The tumor had slightly decreased in size to 22 mm. Computed tomography revealed GCTB in the carpal bones and new bone formation within the tumor. (**f**) Intermixed bone and fibroblast-like spindle cells were observed instead of multinucleated giant cells and intervening mononuclear cells.

is replaced to intermixed bone and fibroblast-like spindle cells.[9] This histological change is also assumed to be one of the reasons for decreasing signal. Therefore, decreasing SI ratio might be relevant to therapeutic effect. The number of the ADC case value was measured was too small; however, three cases showed increasing ADC value and the other three cases showed decreasing ADC value. The ADC value might be limited.

While several adverse events, such as osteonecrosis of the jaw and atypical fracture, have been reported after long-term administration of denosumab for GCTB, this osteoclast inhibition therapy has been reported to be tolerable for continued use as long as the treatment remains consistent with the patient's and clinician's joint goals and there is an absence of excessive toxicity.[20] In addition, one obstacle to surgically managing GCTB is that denosumab treatment renders GCTB less macroscopically and microscopically defined, which makes decisions regarding the extent of any surgical excision more difficult.[21] In our case series, two cases showed local recurrence after denosumab was used as a neo-adjuvant therapy for curettage. Therefore, it is possible that using denosumab should be restricted to cases of GCTB that involve the articular surface or that are located in the trunk, where resection is not feasible. For those unresectable GCTB, transcatheter arterial embolization could be performed as a palliative therapy.[22] In the future, an optimal therapeutic regimen that could include curettage, transcatheter arterial embolization, denosumab, and radiation therapy should be established for GCTB.

There are several limitations to this study. First, this was a retrospective study that consisted of a small number of cases. Second, the follow-up observation period was short. Future studies that carefully document sarcomatous transformation in GCTB in patients who receive denosumab for a long period of time are needed.

Conclusion

We identified changes that occur in GCTB that can be observed as imaging features in patient who received denosumab treatment. The shrinkage of cystic part and bone formation should be regarded as the effectiveness of denosumab treatment despite of no substantial change in the tumor size. These novel findings should be incorporated into treatment decision algorithms.

Conflicts of Interest

The authors declare that they have no conflicts of interest.

References

1. Dufresne A, Derbel O, Cassier P, Vaz G, Decouvelaere AV, Blay JY. Giant-cell tumor of bone, anti-RANKL therapy. Bonekey Rep 2012; 1:149.
2. Cote GM. Rank ligand as a target in musculoskeletal neoplasms. Curr Rev Musculoskelet Med 2015; 8:339–343.
3. Raskin KA, Schwab JH, Mankin HJ, Springfield DS, Hornicek FJ. Giant cell tumor of bone. J Am Acad Orthop Surg 2013; 21:118–126.
4. Roux S, Amazit L, Meduri G, Guiochon-Mantel A, Milgrom E, Mariette X. RANK (receptor activator of nuclear factor kappa B) and RANK ligand are expressed in giant cell tumors of bone. Am J Clin Pathol 2002; 117:210–216.
5. Morgan T, Atkins GJ, Trivett MK, et al. Molecular profiling of giant cell tumor of bone and the osteoclastic localization of ligand for receptor activator of nuclear factor kappaB. Am J Pathol 2005; 167:117–128.
6. Hageman K, Patel KC, Mace K, Cooper MR. The role of denosumab for prevention of skeletal-related complications in multiple myeloma. Ann Pharmacother 2013; 47:1069–1074.
7. Vadhan-Raj S, von Moos R, Fallowfield LJ, et al. Clinical benefit in patients with metastatic bone disease: results of a phase 3 study of denosumab versus zoledronic acid. Ann Oncol 2012; 23:3045–3051.
8. Henry D, Vadhan-Raj S, Hirsh V, et al. Delaying skeletal-related events in a randomized phase 3 study of denosumab versus zoledronic acid in patients with advanced cancer: an analysis of data from patients with solid tumors. Support Care Cancer 2014; 22:679–687.
9. Branstetter DG, Nelson SD, Manivel JC, et al. Denosumab induces tumor reduction and bone formation in patients with giant-cell tumor of bone. Clin Cancer Res 2012; 18:4415–4424.
10. Kang H, Lee HY, Lee KS, Kim JH. Imaging-based tumor treatment response evaluation: review of conventional, new, and emerging concepts. Korean J Radiol 2012; 13:371–390.
11. Higano S, Yun X, Kumabe T, et al. Malignant astrocytic tumors: clinical importance of apparent diffusion coefficient in prediction of grade and prognosis. Radiology 2006; 241:839–846.
12. Bae H, Yoshida S, Matsuoka Y, et al. Apparent diffusion coefficient value as a biomarker reflecting morphological and biological features of prostate cancer. Int Urol Nephrol 2014; 46:555–561.
13. Ueda T, Morioka H, Nishida Y, et al. Objective tumor response to denosumab in patients with giant cell tumor of bone: a multicenter phase II trial. Ann Oncol 2015; 26:2149–2154.
14. Therasse P, Arbuck SG, Eisenhauer EA, et al. New guidelines to evaluate the response to treatment in solid tumors. European Organization for Research and Treatment of Cancer, National Cancer Institute of the United States, National Cancer Institute of Canada. J Natl Cancer Inst 2000; 92:205–216.
15. Chung MH, Lee HG, Kwon SS, Park SH. MR imaging of solitary pulmonary lesion: emphasis on tuberculomas and comparison with tumors. J Magn Reson Imaging 2000; 11:629–637.
16. Wang L, Mazaheri Y, Zhang J, Ishill NM, Kuroiwa K, Hricak H. Assessment of biologic aggressiveness of prostate cancer: correlation of MR signal intensity with Gleason grade after radical prostatectomy. Radiology 2008; 246:168–176.

17. Murphey MD, Nomikos GC, Flemming DJ, Gannon FH, Temple HT, Kransdorf MJ. From the archives of AFIP. Imaging of giant cell tumor and giant cell reparative granuloma of bone: radiologic-pathologic correlation. Radiographics 2001; 21:1283–1309.
18. Pekcevik Y, Kahya MO, Kaya A. Diffusion-weighted magnetic resonance imaging in the diagnosis of bone tumors: preliminary results. J Clin Imaging Sci 2013; 3:63.
19. Sabokbar A, Crawford R, Murray DW, Athanasou NA. Macrophage-osteoclast differentiation and bone resorption in osteoarthrotic subchondral acetabular cysts. Acta Orthop Scand 2000; 71:255–261.
20. Henk HJ, Kaura S. Retrospective database analysis of the effect of zoledronic acid on skeletal-related events and mortality in women with breast cancer and bone metastasis in a managed care plan. J Med Econ 2012; 15:175–184.
21. Gaston CL, Puls F, Grimer RJ. The dilemma of denosumab: Salvage of a femoral head giant cell tumour. Int J Surg Case Rep 2014; 5:783–786.
22. Nakanishi K, Osuga K, Hori S, et al. Transarterial embolization (TAE) of sacral giant cell Tumor (GCT) using spherical parmanent embolic material superabsorbant polymer microsphere (SAP-MS). Springerplus 2013; 2:666.